Published in "Nature 483(): 96–99 , 2012"
which should be cited to refer to this work.

Circadian rhythms govern cardiac repolarization and arrhythmogenesis

Darwin Jeyaraj[1,2], Saptarsi M. Haldar[1], Xiaoping Wan[2], Mark D. McCauley[3], Jürgen A. Ripperger[4], Kun Hu[5], Yuan Lu[1], Betty L. Eapen[1], Nikunj Sharma[1], Eckhard Ficker[2], Michael J. Cutler[2], James Gulick[6], Atsushi Sanbe[6], Jeffrey Robbins[6], Sophie Demolombe[7], Roman V. Kondratov[8], Steven A. Shea[5], Urs Albrecht[4], Xander H. T. Wehrens[3], David S. Rosenbaum[2] & Mukesh K. Jain[1]

Sudden cardiac death exhibits diurnal variation in both acquired and hereditary forms of heart disease[1,2], but the molecular basis of this variation is unknown. A common mechanism that underlies susceptibility to ventricular arrhythmias is abnormalities in the duration (for example, short or long QT syndromes and heart failure)[3–5] or pattern (for example, Brugada's syndrome)[6] of myocardial repolarization. Here we provide molecular evidence that links circadian rhythms to vulnerability in ventricular arrhythmias in mice. Specifically, we show that cardiac ion-channel expression and QT-interval duration (an index of myocardial repolarization) exhibit endogenous circadian rhythmicity under the control of a clock-dependent oscillator, krüppel-like factor 15 (*Klf15*). *Klf15* transcriptionally controls rhythmic expression of Kv channel-interacting protein 2 (KChIP2), a critical subunit required for generating the transient outward potassium current[7]. Deficiency or excess of *Klf15* causes loss of rhythmic QT variation, abnormal repolarization and enhanced susceptibility to ventricular arrhythmias. These findings identify circadian transcription of ion channels as a mechanism for cardiac arrhythmogenesis.

Sudden cardiac death from ventricular arrhythmias is the principal cause of mortality from heart disease worldwide and remains a major unresolved public health problem. The incidence of sudden cardiac death exhibits diurnal variation in both acquired and hereditary forms of heart disease[1,2]. In the general population, the occurrence of sudden cardiac death increases sharply within a few hours of rising in the morning, and a second peak is evident in the evening hours[1]. In specific hereditary disorders, for example, Brugada's syndrome, fatal ventricular arrhythmias often occur during sleep[2]. A common mechanism in both acquired and hereditary forms of heart disease that enhances susceptibility to ventricular arrhythmias is abnormal myocardial repolarization[6]. Clinically, three common types of alterations in myocardial repolarization are evident on the surface electrocardiogram (ECG). First, prolongation of repolarization is seen in acquired disorders (for example, heart failure)[5] and congenital disorders (for example, long QT syndrome)[3]. Second, shortening of repolarization is found in the short QT syndrome[4]. Third, early repolarization is the hallmark ECG finding in Brugada's syndrome[8]. Interestingly, all three modifications of repolarization increase vulnerability to ventricular arrhythmias[6]. Despite rigorous investigation of the biophysical and structural characteristics of ion channels that control myocardial repolarization, the molecular basis for the diurnal variation in occurrence of ventricular arrhythmias remains unknown.

Biological processes in living organisms that oscillate with a periodicity of 24 h are said to be circadian. This cell-autonomous rhythm is coordinated by an endless negative transcriptional–translational feedback loop, commonly referred to as the biological clock[9]. Several physiological parameters in the cardiovascular system such as heart rate, blood pressure, vascular tone, QT interval and ventricular effective refractory period exhibit diurnal variation[10–13]. Recent studies have also identified a direct role for the biological clock in regulating cardiac metabolism, growth and response to injury[14]. Previous studies have also reported that expression of repolarizing ion channels and ionic currents (I_{to}) exhibit diurnal changes[15]. However, a potential link between circadian rhythms and arrhythmogenesis remains unknown. We made the serendipitous observation that *Klf15* expression exhibits endogenous circadian rhythmicity in the heart (Fig. 1a). Gene expression microarrays in hearts of mice that are deficient in *Klf15* led us to identify *KChIP2* (also called *KCNIP2*), the regulatory β-subunit for the repolarizing transient outward potassium current (I_{to}) as a putative target for this factor in the heart. These observations led us to question whether the circadian clock may regulate rhythmic variation in repolarization and alter susceptibility to arrhythmias through *Klf15*.

First, we explored mechanisms through which the circadian clock regulated rhythmic expression of *Klf15* in the heart. Examination of approximately 5 kb of the promoter region of *Klf15* revealed four canonical 'E-box' regions, that is, consensus binding sites for CLOCK and its heterodimer BMAL1 (also called ARNTL), which are essential transcription factors involved in the circadian clock (Supplementary Fig. 1a, inset). Consistent with this finding, *Klf15* luciferase (approximately 5 kb) was activated in a dose-dependent manner by the CLOCK–BMAL1 heterodimer (Supplementary Fig. 1a). To confirm this interaction, we performed chromatin immunoprecipitation (ChIP) and identified rhythmic variation in BMAL1 binding to the *Klf15* promoter in the hearts of wild-type mice, but not in the hearts of *BMAL1*-null mice (Fig. 1b). In accordance with the observations above, the expression of *Klf15* was disrupted in *Bmal1*-null, and *Per2*- and *Cry1*-null hearts (Supplementary Fig. 1b). Thus, our data strongly suggest that the circadian clock directly regulates the oscillation of *Klf15* in the heart.

To determine whether myocardial repolarization and ion-channel expression exhibit 'true' (endogenous) circadian rhythms—that is, oscillate in the absence of external cues such as light—wild-type mice were placed in constant darkness for 36 h and telemetry-based ECG intervals were measured every 2 h for 24 h. Under these conditions, the heart rate and the QT interval corrected to heart rate (QTc) were both rhythmic and exhibited true endogenous circadian rhythmicity (Fig. 1c, d). Next, to examine whether expression of repolarizing ion channels had endogenous circadian rhythms, mice were placed in constant darkness for 36 h, and hearts were collected every 4 h over a 24-h period. The expression of the α-subunit for the transient outward

[1]Case Cardiovascular Research Institute, Harrington Heart and Vascular Institute, Department of Medicine, Case Western Reserve University School of Medicine, Cleveland, Ohio 44106, USA. [2]Heart and Vascular Research Center, MetroHealth campus of Case Western Reserve University, Cleveland, Ohio 44109, USA. [3]Departments of Medicine and Molecular Physiology and Biophysics, Baylor College of Medicine, Houston, Texas 77030, USA. [4]Department of Medicine, Division of Biochemistry, University of Fribourg, CH-1700 Fribourg, Switzerland. [5]Division of Sleep Medicine, Brigham and Women's Hospital and Harvard Medical School, Boston, Massachusetts 02115, USA. [6]Department of Pediatrics, Division of Molecular Cardiovascular Biology, Cincinnati Children's Hospital Medical Center, Cincinnati, Ohio 45229, USA. [7]Institut de Pharmacologie Moléculaire et Cellulaire, UMR CNRS 6097, Université de Nice Sophia Antipolis, 06560 Valbonne, France. [8]Department of Biological, Geological and Environmental Sciences, and Center for Gene Regulation in Health and Disease, Cleveland State University, Cleveland, Ohio, 44115, USA.

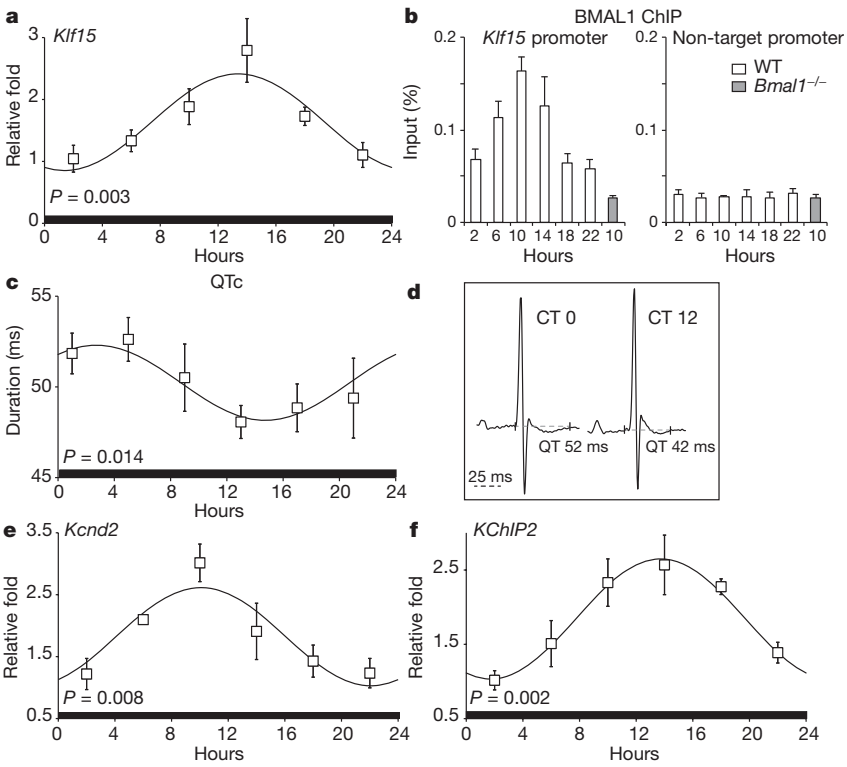

Figure 1 | *Klf15* expression, ECG QTc interval and expression of repolarizing ion channels exhibit endogenous circadian rhythm. **a**, *Klf15* expression exhibits endogenous circadian variation in wild-type (WT) hearts from mice in constant darkness ($n = 4$ per time point). CT, circadian time. **b**, Effect of BMAL1 ChIP on the *Klf15* promoter, showing rhythmic variation in binding of BMAL1 to the *Klf15* promoter in wild-type hearts ($n = 3$ per group). **c**, Duration of ECG QTc interval (ms) in conscious mice exhibits endogenous circadian variation in constant darkness ($n = 4$). **d**, Representative ECGs from conscious mice after 36 h in constant darkness at CT 0 and CT 12. **e**, **f**, Endogenous circadian variation in transcripts for *Kcnd2* and *KChIP2* in wild-type hearts measured every 4 h after 36 h in constant darkness ($n = 4$ per time point). Error bars, mean ± s.e.m.

potassium current (I_{to}), Kv4.2 (encoded by *Kcnd2*) (Fig. 1e), and the regulatory β-subunit, *KChIP2* (Fig. 1f), exhibit endogenous circadian rhythmicity, as did components of the circadian clock in the heart (Supplementary Fig. 2). In contrast, the expression of two other major repolarizing currents in the murine ventricle, Kv1.5 (the α-subunit for the ultra-rapid delayed rectifier potassium current) and Kir2.1 (the α-subunit for the inward rectifier potassium current), did not reveal notable rhythmic variation (Supplementary Fig. 3). In addition, we observed a 24-h rhythm in the oscillation of *Bmal1*, *Klf15* and *KChIP2* after serum shock in cultured neonatal rat ventricular myocytes (Supplementary Fig. 4). These data indicate that myocardial repolarization and the expression of some repolarizing ion channels exhibit an endogenous circadian rhythm.

Next, to elucidate the role of *Klf15* in regulating rhythmic changes in repolarization, we used complementary *in vivo* loss- and gain-of-function approaches in mice. For loss-of-function, a previously described systemic *Klf15*-null mouse was used[16]; for gain-of-function, a cardiac-specific *Klf15* transgenic (*Klf15*-Tg) mouse driven by an attenuated α-myosin heavy chain (α-MHC) promoter was developed (Supplementary Fig. 5). First, we examined whether rhythmic expression of *Kcnd2* or *KChIP2* was altered in the *Klf15*-deficient state. *Kcnd2* expression exhibited altered rhythmic variation in *Klf15*-null mice with reduced expression at zeitgeber time 6 (ZT6), and increased expression at ZT22 compared to wild-type controls (Fig. 2a). KChIP2 expression was devoid of any discernable rhythm in the *Klf15*-null mice and sustained reduction was observed at all time points (Fig. 2b, c and

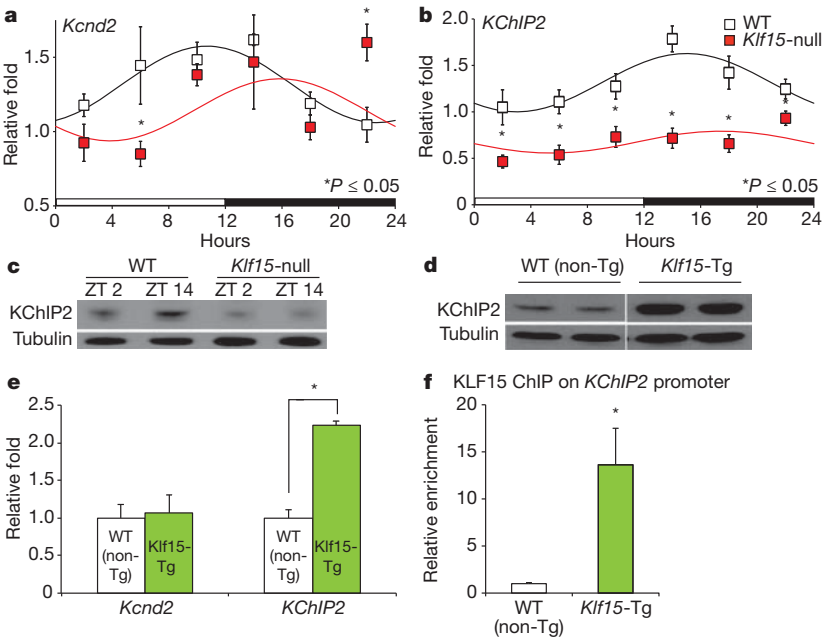

Figure 2 | *Klf15* regulates KChIP2 expression in the heart. **a**, *Kcnd2* mRNA expression exhibits diurnal rhythm in wild-type mice ($P = 0.0023$), but in *Klf15*-null hearts (*P* not significant) the rhythm is abnormal with reduced expression at zeitgeber time 6 (ZT6) and increased expression at ZT22 ($n = 4$ per time point per group). **b**, *KChIP2* mRNA expression exhibits no rhythmic variation in *Klf15*-deficient mice (WT, $P = 0.016$; *Klf15*-null, *P* not significant), with substantial reductions in expression at all time points ($n = 4$ per time point per group). **c**, KChIP2 protein expression exhibits no variation over 12 h in *Klf15*-null hearts. **d**, **e**, *Klf15*-Tg mice hearts express higher levels of KChIP2 mRNA and protein. **f**, Chromatin immunoprecipitation with Flag antibody illustrating enrichment of Flag–KLF15 on the *KChIP2* promoter ($n = 3$ per group). Error bars, mean ± s.e.m., $^*P < 0.05$.

Supplementary Fig. 6a). Next, we examined whether *Kcnd2* or *KChIP2* serve as transcriptional targets for *Klf15* in the heart. Adenoviral overexpression of *Klf15* in neonatal rat ventricular myocytes robustly induced KChIP2 expression but had no effect on *Kcnd2* expression (Supplementary Fig. 6b). Notably, in *Klf15*-Tg hearts, expression of KChIP2 was twofold greater but with no effect on *Kcnd2* expression (Fig. 2d, e). Examination of the *KChIP2* promoter region revealed numerous consensus krüppel-binding sites, that is, C(A/T)CCC (Supplementary Fig. 7a). The activity of *KChIP2* luciferase was induced by full-length KLF15 but not by a mutant that lacked the zinc-finger DNA-binding domain (Supplementary Fig. 7b). To identify the specific *Klf15* binding site, deletion constructs of the *KChIP2* promoter were generated, and transcriptional activity was mapped to the proximal 555 bases (Supplementary Fig. 7a). Mutation of one krüppel-binding site within this region (Δ1) was sufficient to cause complete loss of activity in the full-length *KChIP2* promoter (Supplementary Fig. 7c). Chromatin immunoprecipitation of Flag–KLF15 from *Klf15*-Tg hearts confirmed that KLF15 was enriched on the endogenous *KChIP2* promoter (Fig. 2f). Importantly, the oscillation of several components of the core clock machinery was minimally affected in the *Klf15*-deficient state (Supplementary Fig. 8). In addition, the expression levels of clock genes in *Klf15*-Tg hearts were similar to their controls at ZT6 (Supplementary Fig. 8). This suggested that the endogenous clock is dependent on *Klf15* to orchestrate rhythmic changes in *KChIP2* expression. Consistent with this observation, the expression of *Klf15* (Supplementary Fig. 1b) and *KChIP2* (Supplementary Fig. 9) were altered in a similar fashion in *Bmal1*-null, and *Per2*- and *Cry1*-null mice. These data support the idea that *KChIP2* is a direct transcriptional target for *Klf15* in the heart.

We next examined whether *Klf15*-dependent regulation of *KChIP2* could be responsible for rhythmic day–night variation in myocardial repolarization. Analysis of telemetry-based ECGs revealed that rhythmic QTc interval variation was indeed abrogated in both *Klf15*-null and *Klf15*-Tg mice (Fig. 3a–d). In the *Klf15*-deficient state, the ECG QTc interval was prolonged in the dark phase and failed to oscillate (Fig. 3a, c). This occurred despite *Klf15*-null mice having similar heart rates to their wild-type counterparts (Supplementary Fig. 11). In contrast, the *Klf15*-Tg mice had persistently short QT intervals with no rhythmic day–night variation (Fig. 3b, d). Again, this occurred despite minimal difference in heart rates when compared to wild-type controls (Supplementary Fig. 11). Next, we examined whether transient outward current ($I_{to\ fast}$)-dependent changes in repolarization in isolated myocytes were responsible for the ECG changes mentioned above in *Klf15*-null and *Klf15*-Tg mice. In *Klf15*-null mice, there was a marked reduction in $I_{to\ fast}$ density (Fig. 3e) and prolongation of action potential duration (APD) (Fig. 3g). In contrast, *Klf15*-Tg mice exhibited a substantial increase in $I_{to\ fast}$ density (Fig. 3f) with a dramatic shortening of APD (Fig. 3h). In the *Klf15*-Tg mice, in addition to short QT intervals, we observed ST-segment changes indicative of early repolarization that are similar to ECG findings in Brugada's syndrome[8] (Fig. 3b, arrows). Our data suggest that *Klf15*-dependent transcriptional regulation of rhythmic *KChIP2* expression in murine hearts plays a central part in rhythmic variation in ventricular repolarization.

Next, we examined whether excessive prolongation or shortening of repolarization could alter arrhythmia susceptibility and survival. *Klf15*-null mice show no spontaneous arrhythmias on ECG telemetry, hence we used intracardiac programmed electrical stimulation to examine arrhythmia susceptibility. In contrast to wild-type mice, a marked increase in occurrence of ventricular arrhythmias was seen in *Klf15*-null mice (Fig. 4a). Notably, *Klf15*-Tg mice exhibit spontaneous ventricular arrhythmias on ECG telemetry (Fig. 4b) and succumb to ~35% mortality by 4 months of age (three out of eight deaths in *Klf15*-Tg versus no deaths out of eight in wild-type non-transgenic controls, data not shown). As the *Klf15*-null mice show no evidence of overt ventricular dysfunction, apoptosis or fibrosis[16,17] in the basal state, the enhanced susceptibility to arrhythmias is probably primarily driven by

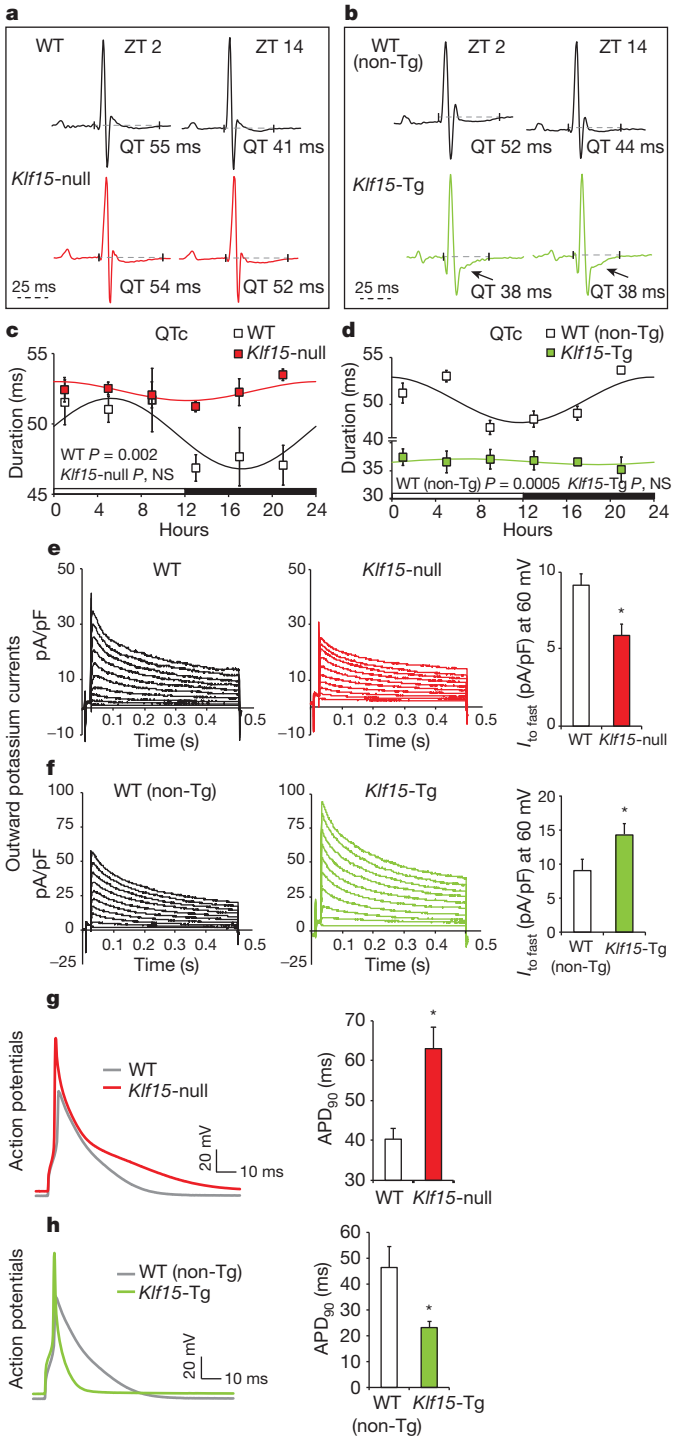

Figure 3 | Deficiency or excess of *Klf15* modulates rhythmic variation in repolarization. **a**, **b**, Representative ECGs from wild-type versus *Klf15*-null mice, and wild-type (non-Tg) versus *Klf15*-Tg mice at ZT2 and ZT14. Note the ST-segment abnormalities in *Klf15*-Tg mice (arrows). **c**, QTc interval exhibits 24-h rhythm in wild-type mice; this rhythm is abrogated with prolonged QTc in the dark phase in *Klf15*-null mice ($n = 4$ for wild type, $n = 4$ for *Klf15*-null). **d**, *Klf15*-Tg mice exhibit persistently short QT intervals with no day–night rhythmic variation compared to wild-type (non-Tg) controls ($n = 3$ for wild type, $n = 4$ for *Klf15*-Tg). **e**, **f**, Representative outward current recordings from all study groups and summary data for the amplitude of $I_{to\ fast}$ measured at 60 mV with an average time of decay of 45 ± 5 ms ($n = 10$ for wild type, $n = 13$ for *Klf15*-null; $n = 14$ for wild type (non-Tg), and $n = 19$ for *Klf15*-Tg). **g**, **h**, Representative ventricular action potentials from all study groups with summary data in bar graphs ($n = 10$ for wild type, $n = 13$ for *Klf15*-null; $n = 14$ for wild type (non-Tg), and $n = 19$ *Klf15*-Tg). Error bars, mean ± s.e.m., $^*P < 0.05$. APD_{90}, action potential duration measured at 90% repolarization.

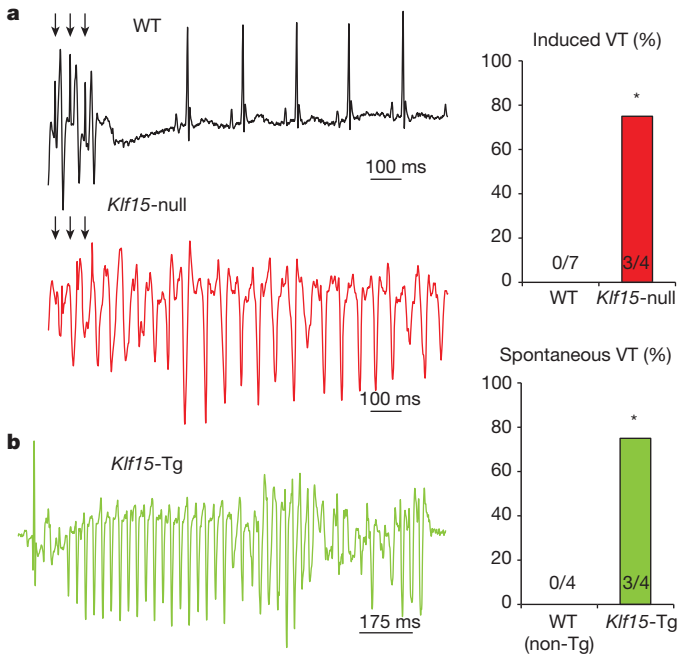

Figure 4 | *Klf15* deficiency or excess increases susceptibility to ventricular arrhythmias. a, Programmed electrical stimulation in wild-type and *Klf15*-null mice. Onset of ventricular tachycardia after premature stimuli is shown (arrows) in *Klf15*-null mice (none of the seven wild-type mice were inducible but three of the four *Klf15*-null mice were inducible; $*P < 0.05$). **b**, Spontaneous ventricular arrhythmia in *Klf15*-Tg mice. (none of the four wild-type mice exhibited spontaneous arrhythmias but three of the four *Klf15*-Tg mice exhibited ventricular arrhythmias; $*P < 0.05$). VT, ventricular tachycardia.

abnormalities in repolarization. Our studies demonstrate that both deficiency and excess of *Klf15* impair temporal variation in cardiac repolarization and greatly increase susceptibility to arrhythmias.

Although our finding of circadian control of KChIP2 by *Klf15* establishes the principle that circadian rhythms may contribute to arrhythmogenesis, we note that *Klf15* minimally affects *Kcnd2* expression that also exhibits circadian rhythm (Fig. 1f). However, *Kcnd2* expression was disrupted in *Bmal1*-null and *Per2*- and *Cry1*-null hearts, and this is indicative of a direct regulation by the circadian clock (Supplementary Fig. 12). Consistent with this observation, cardiomyocytes from *Bmal1*-null mice exhibit marked action potential prolongation due to near-complete elimination of the fast component of the transient outward potassium current (Supplementary Fig. 13). This raises the possibility that additional factors—perhaps components of the circadian clock or unidentified transcriptional regulators—may also affect temporal variation in electrophysiological parameters and arrhythmogenesis. Future studies in cardiac-specific deletion of clock components would be necessary to confirm whether the ion channel rhythms are cell autonomous, and their role in regulating cardiac electrophysiology.

Our study provides the first mechanistic link between endogenous circadian rhythms and the cardiac electrical instability that is most often associated with sudden cardiac death in humans (Supplementary Fig. 14). Specifically, we show that *Klf15*-dependent rhythmic transcription of *KChIP2* regulates the duration and pattern of repolarization and susceptibility to arrhythmias in mice. As the occurrence of sudden cardiac death in acquired and hereditary forms of human heart disease follows a distinct diurnal pattern[1,2], these observations offer new insights into unrecognized triggers of electrical instability in the heart. However, in contrast to murine repolarization, which is largely dependent on I_{to}, human repolarization occurs through a complex interaction of multiple repolarizing ionic currents. Thus, additional studies will be needed to develop a comprehensive understanding of the link between the circadian clock and electrophysiological properties of the human heart. Nevertheless, these data may provide a mechanistic foundation for future efforts to prevent or treat cardiac arrhythmias by modulating the circadian clock through behavioural or pharmacological means.

METHODS SUMMARY

Mice used in the present study, messenger RNA quantification using polymerase chain reaction with reverse transcription (RT–PCR), promoter reporter analysis, western immunoblot analysis, chromatin immunoprecipitation, telemetry ECG and interval analysis, isolated myocyte studies for action potential or I_{to} measurements, *in vivo* electrophysiological studies for arrhythmia susceptibility, cosinor analysis for rhythm assessment, and statistical methods are detailed in the Methods.

Full Methods and any associated references are available in the online version of the paper

1. Muller, J. E. *et al.* Circadian variation in the frequency of sudden cardiac death. *Circulation* **75,** 131–138 (1987).
2. Matsuo, K. *et al.* The circadian pattern of the development of ventricular fibrillation in patients with Brugada syndrome. *Eur. Heart J.* **20,** 465–470 (1999).
3. Goldenberg, I. & Moss, A. J. Long QT syndrome. *J. Am. Coll. Cardiol.* **51,** 2291–2300 (2008).
4. Patel, U. & Pavri, B. B. Short QT syndrome: a review. *Cardiol. Rev.* **17,** 300–303 (2009).
5. Tomaselli, G. F. & Marban, E. Electrophysiological remodeling in hypertrophy and heart failure. *Cardiovasc. Res.* **42,** 270–283 (1999).
6. Antzelevitch, C. Role of spatial dispersion of repolarization in inherited and acquired sudden cardiac death syndromes. *Am. J. Physiol. Heart Circ. Physiol.* **293,** H2024–H2038 (2007).
7. Kuo, H. C. *et al.* A defect in the Kv channel-interacting protein 2 (KChIP2) gene leads to a complete loss of I_{to} and confers susceptibility to ventricular tachycardia. *Cell* **107,** 801–813 (2001).
8. Antzelevitch, C. & Yan, G. X. J wave syndromes. *Heart Rhythm* **7,** 549–558 (2010).
9. Reppert, S. M. & Weaver, D. R. Coordination of circadian timing in mammals. *Nature* **418,** 935–941 (2002).
10. Bexton, R. S., Vallin, H. O. & Camm, A. J. Diurnal variation of the QT interval—influence of the autonomic nervous system. *Br. Heart J.* **55,** 253–258 (1986).
11. Kong, T. Q. Jr, Goldberger, J. J., Parker, M., Wang, T. & Kadish, A. H. Circadian variation in human ventricular refractoriness. *Circulation* **92,** 1507–1516 (1995).
12. Martino, T. A. & Sole, M. J. Molecular time: an often overlooked dimension to cardiovascular disease. *Circ. Res.* **105,** 1047–1061 (2009).
13. Paschos, G. K. & FitzGerald, G. A. Circadian clocks and vascular function. *Circ. Res.* **106,** 833–841 (2010).
14. Durgan, D. J. & Young, M. E. The cardiomyocyte circadian clock: emerging roles in health and disease. *Circ. Res.* **106,** 647–658 (2010).
15. Yamashita, T. *et al.* Circadian variation of cardiac K^+ channel gene expression. *Circulation* **107,** 1917–1922 (2003).
16. Haldar, S. M. *et al.* Klf15 deficiency is a molecular link between heart failure and aortic aneurysm formation. *Sci. Transl. Med.* **2,** 26ra26 (2010).
17. Wang, B. *et al.* The Krüppel-like factor KLF15 inhibits connective tissue growth factor (CTGF) expression in cardiac fibroblasts. *J. Mol. Cell. Cardiol.* **45,** 193–197 (2008).

Acknowledgements We thank A. F. Connors Jr for support, M. Mustar for illustrations, Y. Cui for experimental assistance, and members of the Jain laboratory for discussions. Funding sources: Heart Rhythm Society Fellowship (D.J.); National Institutes of Health grants HL094660 (D.J.), HL066991 (M.D.M.), HL086614 (S.M.H.), American Heart Association postdoctoral grant (N.S.), HL089598, HL091947 (X.H.W.), HL76446 (S.A.S.), HL102241 (K.H.), HL054807 (D.S.R.), HL075427, HL076754, HL084154, HL086548 and HL097595 (M.K.J.); Swiss National Science Foundation grants 31003A/131086 (U.A.) and M01-RR02635 (B.W.H.); Leducq Foundation grants of the ENAFRA Network 07CVD03 (S.D.); and the Centre National de la Recherche Scientifique (S.D.).

Author Contributions D.J. and M.K.J. designed the research; D.J., S.M.H., X.W., M.D.M., J.A.R., Y.L., B.L.E. and M.J.C. carried out the experiments; J.G., A.S., J.R. and R.V.K. contributed critical reagents; D.J., N.S., S.D., R.V.K., S.A.S., U.A., X.H.T.W., D.S.R. and M.K.J. supervised the research; D.J., S.M.H., X.W., M.D.M., J.A.R., K.H., B.L.E., E.F., S.A.S., U.A., X.H.T.W., D.S.R. and M.K.J. analysed and interpreted the data; and D.J. and M.K.J. wrote the manuscript.

METHODS

Mice. All animal studies were carried out with permission, and in accordance with, animal care guidelines from the Institutional Animal Care Use Committee (IACUC) at Case Western Reserve University and at collaborating facilities. Wild-type male mice on C57BL6/J background (Jackson Laboratory) were bred in our facility and used for circadian studies. Mice were housed under strict light–dark conditions (lights on at 6:00 and lights off at 18:00) and had free access to standard chow and water, and were minimally disturbed for 4–6 weeks before the final experiment. Generation of systemic *Klf15*-null mice was as described previously[18]. *Klf15*-null mice have been backcrossed into the C57BL6/J background for over ten generations[18] and the BMAL1 mice were bred as previously described[19]. For *Klf15*-Tg mice, Flag–KLF15 was cloned downstream of an attenuated α-myosin heavy-chain promoter as previously described[20]. This construct was injected into FVB (friend leukemia virus B mouse strain) oocytes, and after germline transmission the mice were examined for expression of the transgene. Wild-type (non-Tg) littermates served as controls. For light–dark experiments, mice were killed with CO_2 inhalation or isoflurane every 4 h for 24 h. For constant dark experiments, mice were placed in complete darkness for 36 h (starting at the end of light phase at ZT12) and hearts were collected every 4 h over a 24-h period.

RNA isolation and RT–PCR analysis: After euthanasia, hearts were collected, washed in cold phosphate buffered saline, the atria removed and the ventricles dissected to the apical and basal regions, and flash frozen in liquid nitrogen. RNA was isolated from the apical regions of frozen heart samples by homogenization in Trizol reagent (Invitrogen) by following the manufacturer's instructions (Invitrogen). RNA was reverse transcribed after DNase treatment (New England Biolabs). RT–PCR was performed using locked nucleic acid (LNA)-based TaqMan approach with primers and probes designed, and their efficiency tested, at the Universal Probe Library (Roche), and with β-actin used as the normalizing gene.

Cell-culture studies. Neonatal rat ventricular myocytes were isolated from 1–2-day-old rat pups and grown under standard conditions[18]. Adenoviral overexpression was performed for 24 h and myocytes were then collected for mRNA and protein analysis. For synchronization, the myocytes were starved in media containing insulin, transferrin and selenium (ITS supplement, Sigma-Aldrich) for 48 h. After this, the myocytes were synchronized with 50% horse serum for 30 min, washed twice with no-serum media and replenished with ITS-containing media. The mouse *Klf15* promoter (approximately 5 kb) was cloned into PGL3-basic (Promega). The rat *KChIP2* luciferase was a gift from P. H. Backx. Mutant constructs of rat *KChIP2* luciferase were generated by PCR-based TOPO cloning (Invitrogen), and site-directed mutagenesis was performed using Quikchange II mutagenesis kit (Agilent Technologies) and confirmed by sequencing. *Klf15* and *KChIP2* luciferase studies were conducted in NIH3T3 cells, and luciferase activity was normalized to protein concentration.

Western immunoblot analysis. For detecting Flag–KLF15, nuclear lysates were prepared using the NE-PER kit following manufacturer's instructions (Thermo Scientific) and probed with anti-Flag antibody (Sigma). For KChIP2 analysis, whole-cell lysates were prepared by homogenizing the basal regions of the hearts in buffer containing Tris-HCl (50 mM, pH 7.4), NaCl (150 mM), NP-40 (1%), sodium deoxycholate (0.25%), EDTA (1 mM), and supplemented with protease and phosphatase inhibitors (Roche). The blots were probed with a mouse monoclonal antibody against KChIP2 (NIH Neuromab), normalized to tubulin (Sigma-Aldrich) and quantified using Quantity One software (Bio-Rad).

ChIP. ChIP was performed with hearts as previously described[21,22]. In brief, hearts were fixed with fresh 1.11% formaldehyde for 10 min, and then by chromatin preparation and sonication (Diagenode). The sonicated chromatin was immunoprecipitated using BMAL1 or Flag antibody bound to Dynabeads (Invitrogen). The relative abundance was normalized to abundance of 28S between the input and immunoprecipitated samples as previously described[21]. Primers that were used for BMAL1 ChIP on the *Klf15* promoter were; forward, 5′-GCCTG AGCATCCTCCCCATCA-3′; reverse, 5′-GGGGCCACCTCTCTGGACTT-3′; and probe, 5′FAM-CCCGCCCAGTGACCATGTCTGCCTGT-3′BHQ1. Non-target primers were; forward, 5′-GCCAATTCACATTTCAACCA-3′; reverse, 5′-GACACAAGGCATTTCAA-3′; and probe, 5′FAM-TGCAAAGGGCTGGA CATGGG-3′BHQ1. Primers that were used for ChIP of Flag–KLF15 on the *KChIP2* promoter were; forward, 5′-GCTCCGCTCTCACTTGCT-3′; and reverse, 5′-GGCTGGCAAGGCTTTTCT-3′.

Telemetry ECG and interval analysis. Mice were implanted with telemetry devices (ETA F20, Data Sciences International) and allowed to recover for at least 2 weeks. ECGs were recorded from conscious mice continuously in their native environment and digital data (PhysioTel, Data Sciences International) were stored for future analysis. Owing to rapid changes in the mouse heart rates, a weighted heart-rate approach was used to assess rhythmic changes in QT interval, and measurements were made every 2 h over a 24-h period. First, the average heart rate was calculated for each hour by digital tracking of the ECG RR intervals (time interval between two consecutive R waves) using the Dataquest analysis software (Data Sciences International). Then, during the first instance within each hour when the average heart rate was present, the QT interval was measured using electronic calipers from two consecutive beats. The QT interval was corrected for heart rate using a previously validated formula for conscious mice $QT/(RR/100)^{1/2}$ (ref. 23). A Cosinor model was applied to assess the 24-h rhythm in QT using a sinusoidal regression function and raw data presented in four hourly blocks for visualization purposes.

Electrophysiological studies in myocytes. Murine ventricular myocytes were isolated using a standard enzymatic dispersion technique following overnight fast as previously described[24]. Myocytes were re-suspended in media 199, allowed to recover and recordings were conducted within several hours on the same day. The conventional whole-cell mode was used to record action potentials and I_{to}. In brief, myocytes were bathed in a chamber that was continuously perfused with Tyrode's solution of the following composition (in mmol l^{-1}): NaCl, 137; KCl, 5.4; $CaCl_2$, 2.0; $MgSO_4$, 1.0; glucose, 10; and HEPES, 10 (pH 7.35). Patch pipettes (0.9–1.5 MΩ) were filled with electrode solution composed of (in mmol l^{-1}): aspartic acid, 120; KCl, 20; NaCl, 10; $MgCl_2$, 2; and HEPES, 5 (pH 7.3). Action potentials were elicited in current-clamp mode by injection of a square pulse of current of 5 ms duration and 1.5–2 times the threshold amplitude. APD was measured at 90% repolarization. To measure I_{to}, cells were placed in Tyrode's solution (as described earlier) containing 1 μM nisoldipine to block calcium current and calcium-activated chloride current, and tetrodotoxin (100 μmol l^{-1}) to block sodium current. Cells were brought from a holding potential of −70 mV to −25 mV for 25 ms. To isolate the fast, transient component of the outward currents, $I_{to\ fast}$, the decay phase of outward potassium currents was fit by the exponential functions of the form:

$$y(t) = A_1 \exp(-t/\tau_1) + A_2 \exp(-t/\tau_2) + A_{ss}$$

where τ_1 is the time constant of decay of the fast, transient component of outward potassium currents; A_1 is the amplitude coefficient of $I_{to\ fast;}$ τ_2 is the time constant of decay of the slow, transient component of the outward currents; A_2 is the amplitude of $I_{to\ slow}$; and A_{ss} is the amplitude coefficient of the non-inactivating steady-state outward potassium current $I_{ss.}$ Consistent with previous studies[25], the time constant of decay of the fast, transient component $I_{to\ fast}$ was 46 ± 5 ms. The measured current amplitudes were normalized to cell capacitance and converted into current densities. All experiments were conducted at 36 °C. Cell capacitance and series resistance were compensated electronically at ~80%. Command and data acquisition were operated with an Axopatch 200B patch-clamp amplifier controlled by a personal computer using a Digidata 1200 acquisition board driven by pCLAMP 7.0 software (Axon Instruments).

Programmed electrical stimulation. Intracardiac programmed electrical stimulation was performed as previously described[26]. In brief, mice were anaesthetized using 1.5% isoflurane in 95% O_2 after an overnight fast. ECG channels were amplified (0.1 mV cm^{-1}) and filtered between 0.05 and 400 Hz. A computer-based data acquisition system (Emka Technologies) was used to record a 3-lead body surface ECG, and up to four intracardiac bipolar electrograms. Bipolar right atrial pacing and right ventricular pacing were performed using 2-ms current pulses delivered by an external stimulator (STG-3008, MultiChannel Systems; Reutlingen). Standard clinical electrophysiologic pacing protocols were used to determine all basic electrophysiologic parameters. Overdrive pacing, single, double and triple extrastimuli, as well as ventricular burst pacing, were delivered to determine the inducibility of ventricular arrhythmias, which was tested twice.

Statistical analysis. A cosinor model was adopted to determine whether there is a substantial 24-h rhythm in each physiological and molecular variable of interest. By pooling data points of all mice, the model fits data to a fundamental sinusoidal function[27]. To determine the coefficients (amplitude and phase) of the sinusoidal function and to see whether there were significant relationships, a mixed model analysis of variance was performed using standard least-square regression and the restricted maximum likelihood method (JMP 8.0, SAS Institute) as previously described[28]. Data are presented as mean ± s.e.m., the Student's *t*-test was used for assessing the difference between individual groups and $P \leq 0.05$ was considered statistically significant.

18. Fisch, S. *et al.* Krüppel-like factor 15 is a regulator of cardiomyocyte hypertrophy. *Proc. Natl Acad. Sci. USA* 104, 7074–7079 (2007); correction **104,** 13851 (2007).
19. Bunger, M. K. *et al.* Mop3 is an essential component of the master circadian pacemaker in mammals. *Cell* **103,** 1009–1017 (2000).
20. Sanbe, A. *et al.* Reengineering inducible cardiac-specific transgenesis with an attenuated myosin heavy chain promoter. *Circ. Res.* **92,** 609–616 (2003).
21. Tuteja, G., Jensen, S. T., White, P. & Kaestner, K. H. *Cis*-regulatory modules in the mammalian liver: composition depends on strength of Foxa2 consensus site. *Nucleic Acids Res.* **36,** 4149–4157 (2008).
22. Ripperger, J. A. & Schibler, U. Rhythmic CLOCK-BMAL1 binding to multiple E-box motifs drives circadian *Dbp* transcription and chromatin transitions. *Nature Genet.* **38,** 369–374 (2006).

23. Mitchell, G. F., Jeron, A. & Koren, G. Measurement of heart rate and Q-T interval in the conscious mouse. *Am. J. Physiol.* **274,** H747–H751 (1998).
24. Libbus, I., Wan, X. & Rosenbaum, D. S. Electrotonic load triggers remodeling of repolarizing current I_{to} in ventricle. *Am. J. Physiol. Heart Circ. Physiol.* **286,** H1901–H1909 (2004).
25. Wagner, S. *et al.* Ca/calmodulin kinase II differentially modulates potassium currents. *Circ. Arrhythm. Electrophysiol.* **2,** 285–294 (2009).
26. van Oort, R. J. *et al.* Ryanodine receptor phosphorylation by calcium/calmodulin-dependent protein kinase II promotes life-threatening ventricular arrhythmias in mice with heart failure. *Circulation* **122,** 2669–2679 (2010).
27. Nelson, W., Tong, Y. L., Lee, J. K. & Halberg, F. Methods for cosinor-rhythmometry. *Chronobiologia* **6,** 305–323 (1979).
28. Hu, K., Scheer, F. A., Laker, M., Smales, C. & Shea, S. A. Endogenous circadian rhythm in vasovagal response to head-up tilt. *Circulation* **123,** 961–970 (2011).